第27卷 第1期
2006年 2月

材 料 热 处 理 学 报
TRANSACTIONS OF MATERIALS AND HEAT TREATMENT

Vol. 27 No. 1
Feburary 2006

TC4钛合金激光熔覆 TiC + M 涂层组织和耐磨性能研究

孙荣禄[1,2]， 杨贤金[2]

(1. 天津工业大学机械电子学院，天津 300160； 2. 天津大学材料科学与工程学院，天津 300072)

摘 要：用 CO_2 激光在 TC4 合金表面熔覆 TiC + Ti 和 TiC + NiCrBSi 金属陶瓷涂层，分析了熔覆层的微观组织，测试了熔覆层的干滑动磨损性能。结果表明，在 TiC + Ti 激光熔覆层中，TiC 颗粒全部溶解，熔覆层的组织是在β-Ti 基体上分布着 TiC 树枝晶；在 TiC + NiCrBSi 激光熔覆层中，TiC 颗粒部分溶解，熔覆层的组织是在γ-Ni 树枝晶和γ-Ni + $M_{23}(CB)_6$ 共晶的基体上分布着细小的 TiC 颗粒和 TiC 树枝晶。TiC + Ti 激光熔覆层的显微硬度在 500～700HV 之间，质量磨损率约为 TC4 合金的 1/3；TiC + NiCrBSi 激光熔覆层的显微硬度在 900～1100HV 之间，质量磨损率约为 TC4 合金的 1/10。

关键词：钛合金； 激光熔覆； TiC 金属陶瓷涂层； 微观组织； 耐磨性能

中图分类号：TG156.99； TG166.5 **文献标识码**：A **文章编号**：1009-6264(2006)01-0096-04

钛合金具有比强度高、耐蚀性能好等优点，是航天、航空、冶金和化学工业等部门中广泛使用的结构材料。但是，钛合金的摩擦系数高、耐磨性能差，且难以润滑，限制了钛合金的应用范围。

激光熔覆陶瓷涂层[1～5]或陶瓷颗粒增强的复合材料涂层[6～11]是提高钛合金表面耐磨性能的有效手段，如 Ayers 等人[1]考察了钛合金表面激光熔覆 TiC 和 WC 涂层的磨损行为，结果表明，熔覆层的耐磨性能与碳化物颗粒的类型、尺寸和加入量密切相关，摩擦系数约为基材的一半。Molin 等人[6]在钛合金表面激光熔覆 BN 和 BN + NiCrCoAlY 涂层，涂层的硬度范围为 800～1200HV，耐滑动磨损性能是钛合金的 10～200 倍。本文通过对 TC4 合金表面 TiC + Ti 和 TiC + NiCrBSi 激光熔覆层的对比研究，揭示了粘结金属种类对 TiC 金属陶瓷激光熔覆层组织、硬度和耐磨性能的影响，旨在为钛合金表面激光熔覆涂层材料的选择奠定基础。

1 试验方法

试验基底材料为在α+β双相区热轧并经 780 ℃退火处理的 TC4(Ti-6Al-4V)合金棒材，熔覆试样尺寸为 ϕ30mm ×20mm。熔覆材料为ω(TiC) ω(Ti) = 1∶2 和ω(TiC) ω(NiCrBSi) = 1∶2(体积比)的机械混合粉末，其中 TiC 粉末的成分为：总含碳量 19.85wt %，游离碳小于 0.2wt %，NiCrBSi 合金粉末的成分(wt %)为：17.0Cr，3.5B，4.0Si，1.0C，< 12Fe，余为 Ni。将基底试样待熔覆表面用砂纸打磨，以去除氧化膜和油污，并用丙酮清洗，采用粘结法将熔覆材料预置在基底试样表面，预置厚度为 1mm。

试验采用 ML-108 型 9kW 横流 CO_2 激光器，熔覆工艺参数为：功率 P = 3～6kW，扫描速度 V = 5～15mm/s，激光束斑直径 D = 6mm。熔覆时用氩气侧吹法保护熔池。

利用 Hitachi S-570 型扫描电镜和 Philips CM12 型透射电镜分析熔覆层的微观组织。利用 HXD-1000 型显微硬度计测量熔覆层的硬度。利用 УТИ ТВ 100 型销-盘式摩擦磨损试验机测试熔覆层的磨损性能，销为多道搭接的激光熔覆试样，尺寸为 ϕ9mm × 15mm，摩擦表面经磨削加工，粗糙度 R_a < 0.2μm，盘为 YG8B 硬质合金(89.5HRA)，尺寸为 ϕ40mm × 10mm。摩擦工作参数为：法向载荷 50N，滑动速度 0.8m/s，滑动距离 540m。用感量为 10^{-5}g 的分析天平测量磨损失重量 Δm，并计算质量磨损率 I($I = \Delta m/L$)。

2 试验结果及分析

2.1 激光熔覆层的宏观形貌

图 1a、b 分别为 TiC + Ti 和 TiC + NiCrBSi 单道激光熔覆试样横截面整体形貌，试样由熔覆层(CL)、基

收稿日期： 2005-04-14； **修订日期**： 2005-06-16

基金项目： 天津市自然科学基金资助项目(043603211)

作者简介： 孙荣禄(1964—)，男，天津工业大学教授，博士，天津大学博士后，主要从事金属材料及表面改性方面的研究工作，发表论文 30 余篇，电话：022-24528671，E-mail：rlsuntjpu@vip.sina.com。

底热影响区(HAZ)和基底三个部分组成。从图中可见,当粘结金属种类不同时,激光熔覆层的形貌存在明显的差别,TiC + Ti 激光熔覆层呈凹陷状,TiC + NiCrBSi 激光熔覆层呈凸起状。激光熔覆层的形貌与激光熔池中熔体的对流运动密切相关,文献[12]指出,激光熔池内熔体对流运动来自于两种不同的机制,一是表面张力梯度引起的强制对流运动,另一是熔池水平温度梯度决定的浮力引起的自然对流运动。当激光熔池中不存在表面活性元素时,两种力作用产生的熔体流动路径的方向在宏观上基本一致,强制对流和自然对流在熔池的右侧耦合成一个宏观上沿顺时针方向流动的主循环对流回路,而在熔池的左侧则沿逆时针方向流动,这种对流运动的结果使熔池形状呈平面状或凹陷状。当激光束移开后,由于基底金属的骤冷作用,可使其几何形状被保留下来。当激光熔池中存在表面活性元素(如 B)时,熔池表面张力将反向,相应的对流结果使熔池呈凸起状。

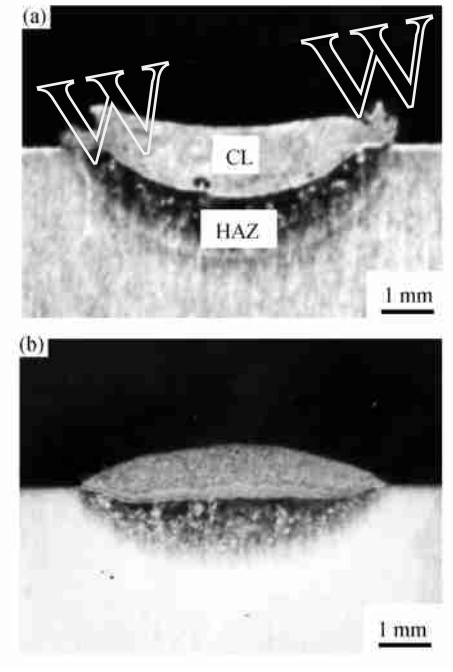

图 1　激光熔覆层横截面形貌

Fig. 1　Morphology of cross-section of laser clad layer (a) TiC + Ti; (b) TiC + NiCrBSi

2.2　激光熔覆层的微观组织

图 2 为 TiC + Ti 激光熔覆层组织 SEM 照片。激光熔覆层的组织是在 Ti 基体上均匀地分布着 TiC 树枝晶。整个激光熔覆层中几乎观察不到 TiC 颗粒,这表明在激光辐照加热过程中 TiC 颗粒发生了溶解,在冷却过程中又以 TiC 树枝晶形式沉淀析出。从图 2b 可以看出,基底热影响区为针状马氏体组织。

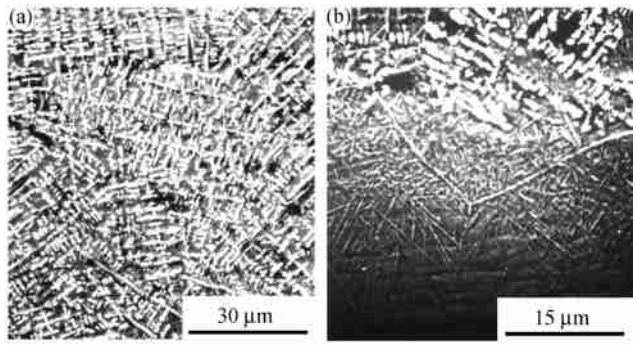

图 2　TiC + Ti 激光熔覆层组织 SEM 照片

Fig. 2　SEM micrographs showing microstructure of TiC + Ti laser clad layer (a) surface layer; (b) bottom layer

图 3a 为 TiC + Ti 激光熔覆层组织 TEM 照片,图 3b、c 分别为 TiC 树枝晶和熔覆层基体的选区电子衍射斑点。对衍射斑点标定表明,熔覆层基体为具有体心立方晶体结构的β-Ti 相。

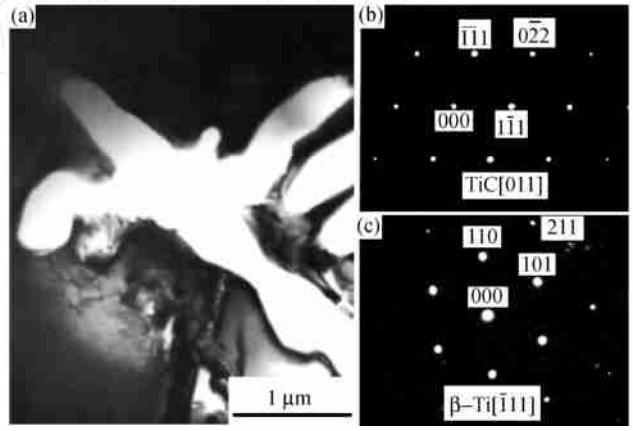

图 3　TiC + Ti 激光熔覆层组织 TEM 照片

Fig. 3　TEM micrographs showing microstructure of TiC + Ti clad layer and correspondine SADPs (a) bright-field image; (b) SADP of TiC; (c) SADP of β-Ti

图 4 为 TiC + NiCrBSi 激光熔覆层组织 SEM 照片。激光熔覆层的组织是在 Ni 基合金的基体上分布着 TiC 颗粒和 TiC 树枝晶,但在熔覆层不同部位 TiC 颗粒和树枝晶的数量存在一定的差别,表层 TiC 颗粒的数量较多,TiC 树枝晶的数量较少,底层则相反,TiC 颗粒的数量较少,TiC 树枝晶的数量较多。分析认为,造成这种现象的原因是底层受到基底钛合金的稀释,高温时 TiC 颗粒向液态钛合金中溶解,冷却时又沉淀析出。

图 5 为 TiC + NiCrBSi 激光熔覆层基体组织 TEM 照片。激光熔覆层基体组织由树枝晶和层片状共晶

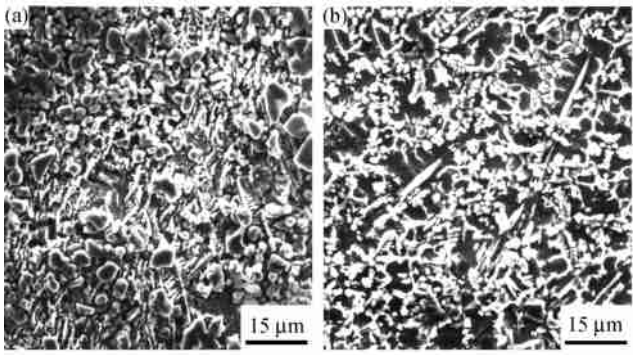

图 4 TiC + NiCrBSi 激光熔覆层组织 SEM 照片

Fig. 4 SEM micrographs showing microstructure of TiC + NiCrBSi laser clad layer (a) surface layer; (b) bottom layer

组成,选区电子衍射分析表明树枝晶为具有面心立方晶体结构的 γ-Ni 固溶体(衍射图略),图 5b、c 分别为共晶组织中亮衬度相和暗衬度相的选区电子衍射斑点,对衍射斑点标定表明,共晶组织中亮衬度相为 γ-Ni 固溶体,暗衬度相为 $M_{23}(CB)_6$。

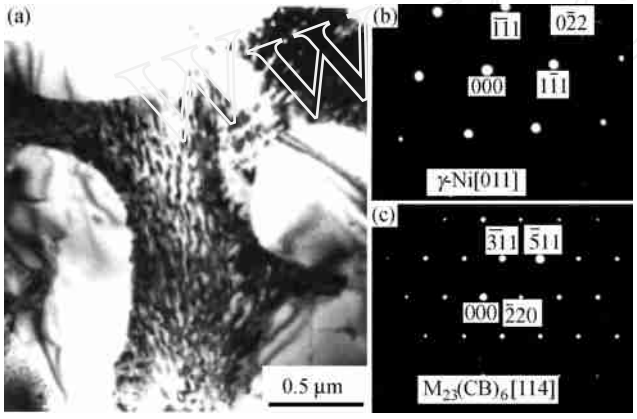

图 5 TiC + NiCrBSi 激光熔覆层基体组织 TEM 照片

Fig. 5 TEM micrographs showing γ-Ni dendrites and γ-Ni + $M_{23}(CB)_6$ eutectic and corresponding SADPs (a) bright-field image; (b) SADP of γ-Ni; (c) SADP of $M_{23}(CB)_6$

由上述分析可见,当粘结金属种类不同时,激光熔覆层中 TiC 相的形态存在明显的差别,在 TiC + Ti 激光熔覆层中 TiC 颗粒全部溶解,熔覆层的组织是在 β-Ti 基体上分布着 TiC 树枝晶。在 TiC + NiCrBSi 激光熔覆层中 TiC 颗粒发生了部分溶解,熔覆层的组织是在 γ-Ni 树枝晶和 γ-Ni + $M_{23}(CB)_6$ 共晶的基体上分布着细小的 TiC 颗粒和 TiC 树枝晶。

2.3 激光熔覆层的硬度和耐磨性能

图 6 为 TiC + Ti 和 TiC + NiCrBSi 激光熔覆层显微硬度沿层深方向分布曲线,可见,TiC + Ti 激光熔覆层的硬度在 500～700HV 之间,约为 TC4 合金(300～320HV)的 2 倍;TiC + NiCrBSi 激光熔覆层的硬度在 900～1100HV 之间,约为 TC4 合金的 3～4 倍。

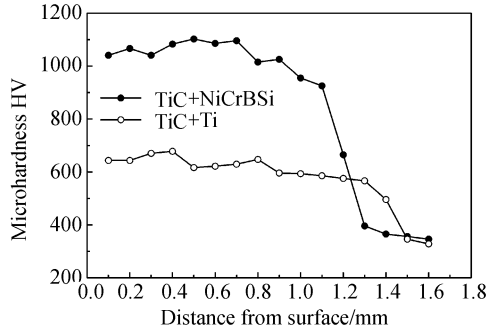

图 6 激光熔覆层显微硬度沿层深方向分布曲线

Fig. 6 Profile of microhardness of laser clad layer

表 1 列出了 TiC + Ti、TiC + NiCrBSi 激光熔覆层及 TC4 合金的质量磨损率,可见,两种激光熔覆层均明显地提高了 TC4 合金的表面耐磨性能,TiC + Ti 激光熔覆层的质量磨损率约为 TC4 合金的 1/3,TiC + NiCrBSi 激光熔覆层的质量磨损率约为 TC4 合金的 1/10。

表 1 激光熔覆层的质量磨损率

Table 1 Mass loss rate of laser clad layer

Material	Mass loss/ mg	Mass loss rate/(mg/m)
TiC + Ti	8.26	1.53×10^{-2}
TiC + NiCrBSi	2.52	4.67×10^{-3}
TC4	22.34	4.47×10^{-2}

图 7a、b 分别示出了 TiC + Ti 和 TiC + NiCrBSi 激光熔覆层的磨损表面形貌。可见,TiC + Ti 激光熔覆层的磨损表面存在较深的犁沟和粘着撕脱痕迹,而 TiC + NiCrBSi 激光熔覆层的磨损表面比较平坦,磨痕细密。两种激光熔覆层磨损形貌的差别与熔覆层的

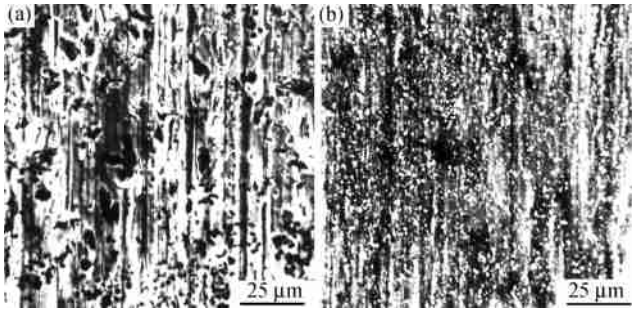

图 7 激光熔覆层的磨损表面形貌

Fig. 7 SEM micrographs showing the worn surface of laser clad layer (a) TiC + Ti; (b) TiC + NiCrBSi

硬度密切相关,TiC + Ti 激光熔覆层的硬度较低,对磨盘表面微凸体在摩擦载荷的作用下压入其表面,进而产生犁削作用,而且由于钛是高活性金属元素,在摩擦热的作用下,与对磨偶件易于产生粘着,当摩擦副相对运动时,粘着接点将被剪断,产生局部撕脱现象。而 TiC + NiCrBSi 激光熔覆层是在 Ni 基合金的基体上分布着大量的 TiC 颗粒,熔覆层的硬度极高,对磨盘表面微凸体对其犁削作用较弱,磨痕细而浅。

3　结论

(1) TiC 金属陶瓷激光熔覆层的宏观形貌与粘结金属的种类密切相关,TiC + Ti 激光熔覆层呈凹陷状,TiC + NiCrBSi 激光熔覆层呈凸起状。

(2) 在 TiC + Ti 激光熔覆层中,TiC 颗粒全部发生了溶解,熔覆层的组织是在β-Ti 基体上分布着 TiC 树枝晶。在 TiC + NiCrBSi 激光熔覆层中,TiC 颗粒发生了部分溶解,熔覆层的组织是在 γ-Ni 树枝晶和 γ-Ni + $M_{23}(CB)_6$ 共晶的基体上分布着细小的 TiC 颗粒和 TiC 树枝晶。

(3) TiC + Ti 激光熔覆层的显微硬度在 500～700HV 之间,质量磨损率约为 TC4 合金的 1/3。TiC + NiCrBSi 激光熔覆层的显微硬度在 900～1100HV 之间,质量磨损率约为 TC4 合金的 1/10。

参　考　文　献

[1] Ayers J D. Wear behavior of carbide-injected titanium and aluminum alloys[J]. Wear, 1984, 97:249 - 266.

[2] Mridha S, Baker T N. Composite laser formation on Ti-6Al-4V surfaces by laser treatment using preplaced SiC powder[J]. Surface Engineering, 1997, 13(3):233 - 237.

[3] Mehlmann A, Dirnfeld S F, Minkoff I. Laser-melt injection of B_4C on titanium[J]. Surface and Coatings Technology, 1990, 42:275 - 281.

[4] 陈赤囡, 苏　梅. TC9 激光熔覆 TiN 涂层的组织与耐磨性能研究[J]. 北京航空航天大学学报, 1998, 24(3):253 - 255.
Chen Chi-nan, Su Mei. Study on microstructure and abrasive resistance of laser cladding TiN surface alloyed TC9[J]. Journal of Beijing University of Aeronautics and Astronautics, 1998, 24(3): 253 - 255.

[5] 李　平, 邓永瑞. 钛合金表面激光熔覆氧化锆陶瓷涂层的显微组织[J]. 稀有金属材料与工程, 1995, 24(4):19 - 24.
Li Ping, Deng Yong-rui. Microstructure of ceramic coating of laser coating ZrO_2 on titanium alloy [J]. Rare Metal Materials and Engineering, 1995, 24(4): 19 - 24.

[6] Molian P A, Hualun L. Laser cladding of Ti-6Al-4V with BN for improved wear performance[J]. Wear, 1989, 130:337 - 352.

[7] 孙荣禄, 杨贤金. 激光熔覆原位合成 TiC-TiB_2/Ni 基金属陶瓷涂层的组织和摩擦磨损性能[J]. 硅酸盐学报, 2003, 31(12):1221 - 1224.
Sun Rong-lu, Yang Xian-jin. Microstructure, friction and wear properties of in situ synthesized TiC-TiB_2/Ni-based metallic ceramic coating by laser cladding [J]. Journal of the Chinese Ceramic Society, 2003, 31(12):1221 - 1224.

[8] 孙荣禄, 刘　勇, 杨德庄. TC4 合金及其表面 TiC_p/Ni 基合金激光熔覆层的摩擦磨损性能[J]. 摩擦学学报, 2003, 23(6):457 - 462.
Sun Rong-lu, Liu Yong, Yang De-zhuang. Friction and wear properties of TiC_p/Ni-based laser clad layer on TC4 alloy[J]. Tribology, 2003, 23(6):457 - 462.

[9] Mridha S, Baker, T N. Metal matrix composite laser formed by laser processing of commercial purity Ti-SiC_p in nitrogen environment[J]. Materials Science and Technology, 1996, 12: 595 - 602.

[10] 张　松, 张春华, 王茂才, 等. Ti6Al4V 表面激光熔覆原位自生 TiC 颗粒增强钛基复合材料及摩擦磨损性能[J]. 金属学报, 2001, 37(3):315 - 320.
Zhang Song, Zhang Chun-hua, Wang Mao-cai, et al. An in situ formed TiC particle reinforcement composite coating induced by laser melting on surface of alloy Ti6Al4V and its wearing performance[J]. Acta Metallurgica Sinica, 2001, 37(3):315 - 320.

[11] 武万良, 黄文荣, 杨德庄, 等. Ti-6Al-4V 合金基体上激光熔覆 Ti-TiC 粉末的显微组织[J]. 激光技术, 2003, 27(4):307 - 310.
Wu Wan-liang, Huang Wen-rong, Yang De-zhuang, et al. Microstructure of laser clad Ti + TiC powders on Ti-6Al-4V alloy substrate[J]. Laser Technology, 2003, 27(4):307 - 310.

[12] 刘江龙, 邹至荣, 苏宝熔. 高能束热处理[M]. 北京: 机械工业出版社, 1997: 144 - 158.

wear resistance; laser cladding

Grain refinement of AZ91HP magnesium alloy treated by vacuum laser melting

GAO Ya-li[1], WANG Cun-shan[1], LIU Hong-bin[1], YAO Man[2] (1. Key State Laboratory for Materials Modification, Dalian University of Technology, Dalian 116023 China; 2. Materials Department of Dalian University of Technology, Dalian 116023 China)

Trans Mater Heat Treat, 2006, 27(1): 92～95, figs 7, tabs 1, refs 7.

Abstract: AZ91HP magnesium alloy was treated by vacuum laser melting. The results show that microstructure of the laser melting zone consists of α-Mg and β-$Mg_{17}Al_{12}$ phases. The amount of β-$Mg_{17}Al_{12}$ phase in the melted zone is more than that of the as-received Mg alloy and increases with decreasing of laser scanning speed. The microstructure in the melted zone grows in the form of dentrite shape, and its second dendrite arm spacing increases along the depth of the melted layer due to non-uniformity of melt composition and crystallizing parameters. The second dendrite arm spacing decreases with increasing of scanning speed. The refining of grains is in favor of increasing of magnesium alloy plasticity.

Key words: laser melting; magnesium alloy; grain refinement; plasticity

Microstructure and wear resistance of laser clad TiC + Ti and TiC + NiCrBSi composite layers on Ti-6Al-4V alloy

SUN Rong-lu[1,2], YANG Xian-jin[2] (1. School of Mechanical and Electronic Engineering, Tianjin Polytechnic University, Tianjin 300160, China; 2. School of Materials Science and Engineering, Tianjin University, Tianjin 300072, China)

Trans Mater Heat Treat, 2006, 27(1): 96～99, figs 7, tabs 1, refs 12.

Abstract: Laser cladding of Ti-6Al-4V alloy with TiC + Ti and TiC + NiCrBSi powders was performed. The microstructure of the two types of laser clad layers was characterized using SEM and TEM, and the dry sliding wear property of the coatings was evaluated using pin-on-disc wear test machine. The results show that all TiC particles are dissolved to form a microstructure of TiC dendrites in β-Ti matrix in the clad layer for TiC + Ti laser clad coating. For TiC + NiCrBSi laser clad coating, parts of TiC particles are dissolved to form a microstructure of TiC particles and fine TiC dendrites in the matrix of γ-Ni dendrites and γ-Ni + $M_{23}(CB)_6$ eutectics in the clad layer. The microhardness of TiC + Ti laser clad layer is in a range of 500～700HV with the wear mass loss ratio being third of that of Ti-6Al-4V alloy. The microhardness of TiC + NiCrBSi laser clad layer is in a range of 900～1100HV with the wear mass loss ratio being an order of magnitude less than that of Ti-6Al-4V alloy.

Key words: titanium alloys; laser cladding; TiC metal/ceramics coating; microstructure; wear resistance

Study on phases of boronized coating on chromium electroplated carbon steel

LI Fu-min[1,2], LIU Xin-sheng[1], WANG Shu-huan[1] (1. Metallurgy and Energy Sources School, Hebei Polytechnic University, Tangshan 063009, China; 2. Materials and Metallurgy School, Northeastern University, Shenyang 110004, China)

Trans Mater Heat Treat, 2006, 27(1): 100～103, figs 9, tabs 3, refs 10.

Abstract: Chromium boride has been obtained by salt-bath boriding on chromium electroplated 45 carbon steel. The phase of the boronized layer was analyzed by microscope, XRD and EPMA. The results show that the boronized layer has multi-layer phase structure of CrB_2 and CrB. To obtain better layer, the boronizing process is controlled at 900～1000 ℃ for 4～6h.

Key words: layer; chromium boride; multi-layer phase structure

Investigation of Mo-Cr alloying layer on Q235 steel prepared by double glow discharge technology and different heat treatment

XU Jin-yong[1,2], LIU Yan-ping[1], WANG Jian-zhong[1], KUI Xiao-yun[1], GAO Yuan[1], XU Zhong[1] (1. Taiyuan University of Technology, Taiyuan 030024, China; 2. Guilin University of Electronic Technology, Guilin 541004, China)

Trans Mater Heat Treat, 2006, 27(1): 104～107, figs 5, tabs 0, refs 11.

Abstract: Different heat treatment processes and the microstructures and mechanical properties of Mo-Cr infiltration layer on Q235 steel prepared by double glow discharge technology were studied. The results show that, after the Q235 steel samples were treated by Mo-Cr infiltration + carbonization + quenching + cryogenic processing + low tempering, the carbides of the steel alloying layer are compact, uniform and disperse, the dimension of the surface carbides are less than 1μm, the surface hardness is up to 1600HV. The abrasion testes results of the samples treated by different processes indicate that, the ratios of relative wear resistance are 1, 1.32, 1.6 and 2.74 respectively, for the processes of carbonization + quenching + tempering at low temperature, Mo-Cr metallic cementation + plasma nitriding, Mo-Cr metallic cementation + carbonization + quenching + tempering at low temperature, Mo-Cr metallic cementation + carbonization + quenching + cryogenic processing for 2h + tempering at low temperature.

Key words: Mo-Cr metallic cementation; surface alloying; cryogenic treatment; plasma nitriding; carbide

Oxidation kinetics of Al-Si coating on superalloy K4104

YANG Shi-wei, LOU Jin, JIANG Yan, LIU Hai-tao (Harbin Engineer University, Harbin 15001, China)

Trans Mater Heat Treat, 2006, 27(1): 108～111, figs 5, tabs 3, refs 7.

Abstract: Al-Si coatings on nickel-base superalloy K4104 were prepared by slurry process. Three kinds of Al-Si coatings were obtained by changing content of CrO_3 in agglomerant. High temperature oxidation resistance of these coatings were studied by high temperature test at 1000 ℃ for 200h in static air. Morphology of oxide scales was studied by SEM and their composition was analyzed by EDX. Oxidation kinetics and oxidation kinetic equations were obtained